Title	Variable repetition frequency asynchronous optical sampling method without a feedback loop
Author(s)	Nagakubo, A.; Kanai, K.; Tamura, H. et al.
Citation	AIP Advances. 2022, 12, p. 045323
Version Type	VoR
URL	https://hdl.handle.net/11094/93314
rights	This article is licensed under a Creative Commons Attribution 4.0 International License.
Note	

Variable repetition frequency asynchronous optical sampling method without a feedback loop

A. Nagakubo ✉ ; K. Kanai; H. Tamura; A. Tange; H. Ogi

Check for updates

CHORUS

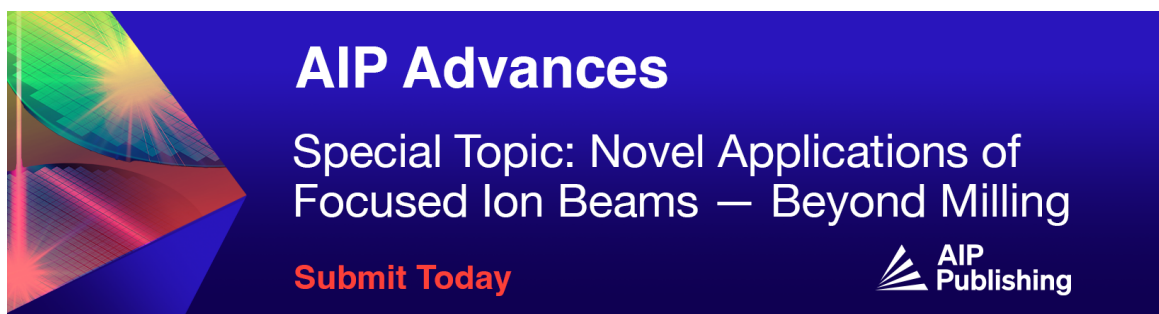View Online   Export Citation   CrossMark

Variable repetition frequency asynchronous optical sampling method without a feedback loop

A. Nagakubo,[a] K. Kanai, H. Tamura, A. Tange, and H. Ogi

AFFILIATIONS

Graduate School of Engineering, Osaka University, Suita, Osaka 565-0871, Japan

[a]Author to whom correspondence should be addressed: nagakubo@prec.eng.osaka-u.ac.jp

ABSTRACT

The ultrafast pump–probe measurement represents a key technique to study fs–ps dynamics. The asynchronous optical sampling (ASOPS) method realizes fast and long time-range measurement with high time resolution using different repetition frequency pump–probe light pulses. The frequency difference Δf is an important parameter, as it dictates the measurement time and time resolution. However, usual ASOPS measurements require a complex and precise stabilizer to control Δf or it is difficult to change Δf. In this study, we use two free-running titanium/sapphire pulse lasers to develop a variable repetition frequency ASOPS (VRF-ASOPS) method without a stabilizer or feedback loop, where we can easily alter Δf by changing the cavity length of the probe light laser. To detect the coincidences of the pump–probe light pulses, we cause the instantaneous reflectivity change in a 100 nm platinum film by irradiating the pump light and observe it by the probe light. We use this signal as the trigger signal to directly determine Δf, which enables us to average and convert the measured responses without a stabilizer or feedback loop. Using this VRF-ASOPS system, we obtain pulse echo signals and 100 GHz Brillouin oscillations, which are equivalent to those measured by the mechanical delay line method, confirming the validity of our developed method.

The ultrafast pump–probe measurement with fs-pulse lasers enables observation of optical,[1] electrical,[2] magnetic,[3–5] and phononic[6,7] dynamics in the order of fs–ps. These time-resolved measurements require controlling the delay time between pump–probe light pulses. The mechanical delay line (MDL) system, which comprises corner reflectors and stage controllers, is often employed and achieves fs–ps order time resolution. However, high time resolution requires longer measurement times. Furthermore, the MDL system requires a long delay line to observe ns-order responses, which requires a large measurement system.[8] For fast measurement, the electronically controlled optical sampling (ECOPS) method can be used, where the delay time of pulses is controlled in the laser cavity by piezoelectric-transducer (PZT) stages.[9,10] However, the observation time range remains restricted due to the short length of the PZT stage. The asynchronous optical sampling (ASOPS) method realizes fast and long time-range measurement by using two lasers with slightly different repetition frequencies (f_r and $f_r - \Delta f$).[11] The arrival time of the pump and probe pulses changes with $\sim \Delta f / f_r^2$ for each pulse, which corresponds to the principal time resolution. $1/\Delta f$ corresponds

to the measurement time to obtain the full temporal response between the pump pulses. Typical values of f_r and Δf are ~80–1000 MHz and 1–10 kHz, respectively. Therefore, the ASOPS system enables long time-range (1–10 ns) and fast measurement (~s) in the time resolution on the order of ~ps and has been applied for THz imaging,[12] studying acoustic properties,[13–16] exciting voltage pulses,[17,18] and cell imaging by GHz ultrasonics.[19–21]

The key aspects of the ASOPS method are the frequency difference Δf and how to stabilize it. A smaller Δf yields higher time resolution and longer measurement time, while a larger Δf has the inverse effect. Moreover, the stability, precision, and accuracy of Δf affect the actual time resolution and reliability of measurement. In conventional ASOPS methods, Δf is controlled by synthesizers[22–24] or a phase-locked loop with photodiodes[25,26] for THz time-domain spectroscopy (TDS). Bartels et al. employed 1 GHz repetition frequency titanium (Ti)/sapphire pulse lasers for THz TDS[27–29] and phonon dynamics,[30,31] achieving 45 fs time resolution with $\Delta f = 2$ kHz.[32,33] A rubidium frequency standard and fiber laser likewise enables ASOPS measurement with $f_r \sim 50$ MHz and $\Delta f = 5$ Hz.[34] However, these methods require controlling the

repetition frequencies with a complex and precise feedback system. Without such a stabilizer, the arbitrary-detuning ASOPS (AD-ASOPS) method was developed using free-running lasers, whose repetition frequencies can be largely different (Δf = 20–70 MHz). The coincidence of the pump and probe pulses is detected by the light-interference effect in an optical fiber, which is used as the trigger signal to acquire and interpolate temporal responses within the coincidence period.[35–37] A single fiber laser without an MDL can yield temporal responses similar to those obtained by ASOPS methods; the optical sampling by cavity tuning (OSCAT) method uses a fiber laser for pump and probe lights with adding a long optical-fiber delay line into one of the light paths. At a certain time, different pulses in the pulse train arrive at a specimen, and their time differences can be changed by sweeping the repetition frequency of the laser.[38,39] The self-triggered ASOPS method utilizes a multiplexed mode-locked fiber laser, where the repetition frequencies of the pump–probe light pulses irradiated from the laser are detuned in an optical fiber depending on the group-velocity dispersion and birefringence.[40] These methods realize fast and long time-range measurements and high time-resolution. However, previous ASOPS methods require a complex system, tightly tuned lasers, or specially designed programs, which makes ASOPS methods difficult and expensive. It is also important to change Δf—the time resolution and measurement time—which cannot be achieved by low cost fixed cavity lasers. A variable Δf system without a feedback loop allows easy application of the ASOPS method and optimization of the system depending on the objectives and purposes.

In this study, we develop a variable repetition frequency ASOPS (VRF-ASOPS) method with a platinum (Pt) trigger specimen using two free-running Ti/sapphire pulse lasers. To make an ASOPS system without a stabilizer or feedback loop, we use a 100 nm Pt thin film as a trigger specimen. We directly measure Δf from the trigger signal and average the responses for each pulse pair using a developed real-time processing program. Finally, we measure and compare acoustic pulse echoes and 100 GHz ultrasounds obtained by the MDL and VRF-ASOPS methods in the range of Δf = 1–4 kHz, confirming the validity of the VRF-ASOPS method with a Pt trigger specimen.

We use two Ti/sapphire pulse lasers from Mai Tai (Spectra-Physics) and Mira (COHERENT) as pump and probe light pulses, respectively. Their repetition frequency f_r, wavelength, and pulse width are ~80 MHz, 800 nm, and 100–130 fs, respectively. f_r of the probe light pulses can be freely changed between 80 ± 0.1 MHz by a PZT stage in the cavity, enabling us to change Δf as well. However, because the lasers are free-running, Δf varies with time and we directly measure Δf using a 100 nm Pt thin film as the trigger specimen; we focus the pump–probe light pulses on the trigger specimen, as shown in Fig. 1, causing and detecting instantaneous hot-electron excitation as the trigger signal. We obtain the temporal responses from a measurement specimen and convert each response by the corresponding Δf measured from the trigger specimen at the same time, enabling ASOPS measurement without a stabilizer or feedback loop. To obtain the trigger signal, we use the same optical system in the same way to obtain the responses of the measurement specimen, simplifying our method.

We convert the wavelength of the probe light pulses into 400 nm by a second harmonic generator (SHG) with a β-BaB$_2$O$_4$
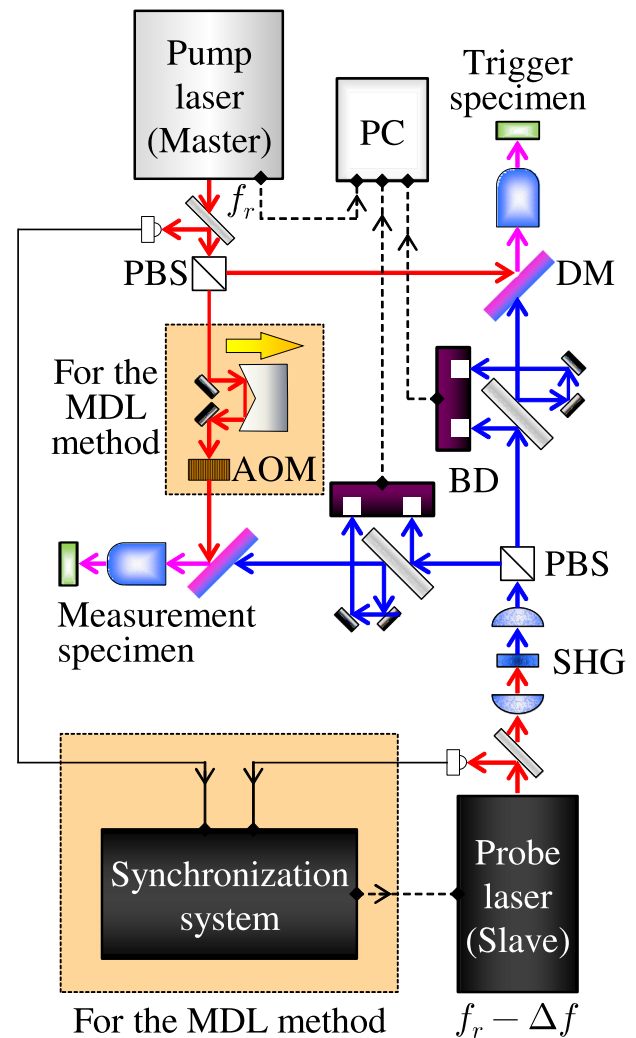
FIG. 1. VRF-ASOPS system without a feedback loop. The repetition frequency of the probe light pulses can be changed by the PZT stage in the laser cavity. Both pump and probe lasers are free-running. For MDL measurement, we include a delay line and synchronizer.

crystal. Pump–probe light pulses are split into trigger- and measurement-specimen paths by polarization beam splitters (PBSs). To overlap them, we use dichroic mirrors (DMs), which reflect and transmit 800 and 400 nm light, respectively. Both pump–probe light pulses enter the specimens perpendicularly through objective lenses. We use a 100-magnification apochromatic lens (Nikon, CFI TU Plan Apo EPI 100×) for the trigger specimen. To extract the reflectivity changes caused by the pump light pulse, we use balanced detectors (BDs) (Newport, 2107-FS-M). We correct responses obtained from the trigger and measurement specimens and pulse signals of the pump light by a 16-bit and 1 GS/s digitizer (National Instruments; NI, PXIe-5764) connected to a Xeon 8-cores personal computer (PC) controller (NI, PXIe-8880) through an 8 GB/s bandwidth chassis (NI, PXIe-1082).

To compare with the MDL measurement, we include corner reflectors with a stage controller and an acoustic optical modulator (AOM) in the measurement-specimen path of the pump light. During the MDL measurement, we modulate the pump light pulses as 100 kHz for lock-in detection. We further synchronize the two lasers by a synchronization system (COHERENT, Synchrolock-AP), where pump–probe light pulses are used as master and slave lasers, respectively.[41]

First, we demonstrate the validity of the Pt-trigger ASOPS method. A Pt thin film is useful and suitable to obtain trigger signals because pulsed-laser absorption in metal causes excitation of hot electrons on the order of fs, leading to very fast and large reflectivity changes. Previous ASOPS methods utilized SHG or sum-frequency generation,[25,27,34,36] a double-balanced mixer with two photodiodes,[28,31] two-photon absorption in a photodiode,[29,32,33] and light interference in an optical fiber[35,42,43] to obtain the trigger signal. A recent AD-ASOPS method achieves ~200 fs time resolution to determine the delays between each pump–probe pulse pair using photodetectors and a specially designed electronic system.[44] These complex systems require different optics and electronics. In contrast, our method uses the same optics as the usual MDL method without the delay line, AOM, and synchronizer as shown in Fig. 1. Note that we still require fast digitizer detectors as well as other methods. This system also enables ASOPS measurement using a conventional oscilloscope and the same optics with off-line processing; we have just recorded every response during the measurement, and converted and averaged the responses later, which are much cheaper than a frequency stabilizer or synthesizer. Recent ASOPS methods propose more complex and higher time resolution methods, however, that is not so important in GHz-range measurement because, for example, cell imaging uses 10–100 GHz ultrasound,[19–21] where 1–10 ps time resolution is enough. Convenient ASOPS measurement must contribute to wider applied physics, such as 1–100 GHz-range biosensors,[45] spin-wave imaging,[46] phase-transition monitoring,[47] and resonator evaluation.[48]

Pt is an excellent trigger specimen owing to its chemical stability and high melting point. Moreover, the trigger metal must possess lower and higher reflectivity for 800 nm pump light and 400 nm probe light, respectively (R_{800} and R_{400}). The penetration depth of the pump light L_{800} must be short to concentrate the absorption energy near the surface. Therefore, we define an absorption–reflection factor (AR-factor) Ψ as

$$\Psi = \frac{1 - R_{800}}{L_{800}} R_{400} = R_{400} \frac{1 - R_{800}}{800/4\pi\kappa_{800}}$$
$$\propto R_{400}(1 - R_{800})\kappa_{800}, \qquad (1)$$

where κ_{800} is the extinction coefficient of the 800 nm pump light. We evaluate $R_{400}(1 - R_{800})\kappa_{800}$ values for typical metals and show the relation between their melting points in Fig. 2(a). Among these, Pt has a high AR-factor, melting point, and chemical stability, enabling a high signal-to-noise ratio (SNR) trigger signal in the long term.

We obtain high intensity and fast trigger signals as shown in Fig. 2(b) with $\Delta f \sim 1.39$ kHz. The powers of pump and probe lights were about 50 and 20 mW, respectively, and gain G was 10^3. The output voltage change ΔV_{out} was about 0.12 V, which corresponds to the actual reflectivity changes $\Delta R_{400}/R_{400}$ of the order of 10^{-3}; the output voltage is calculated by $\Delta V_{out} = \Delta P R_f G$, where ΔP is the
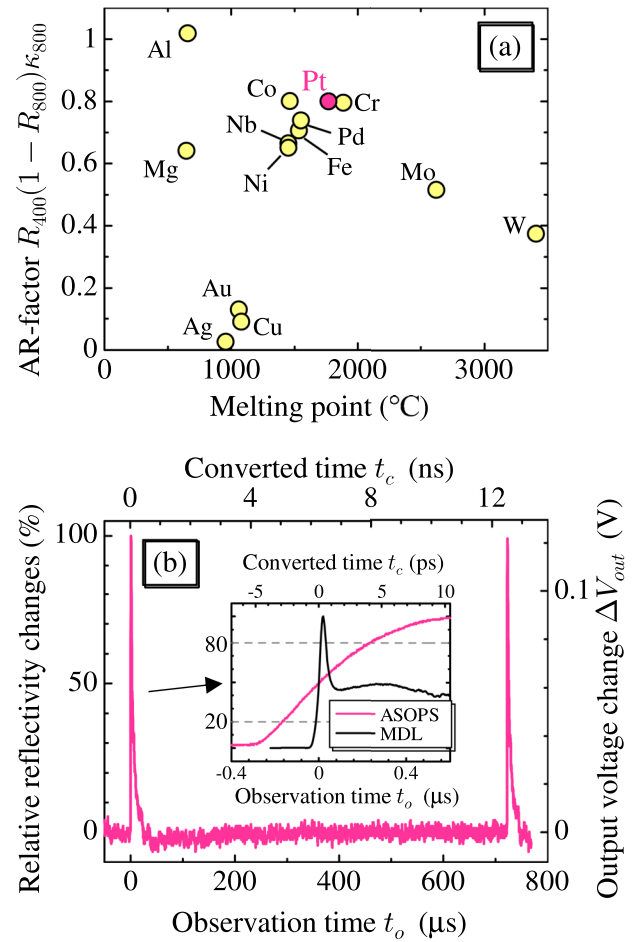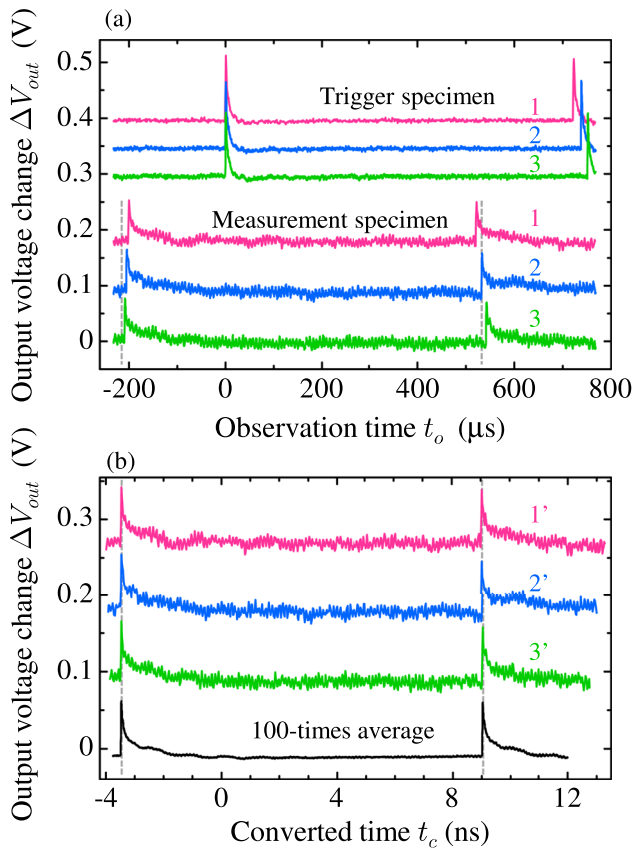

FIG. 2. (a) Relation between melting point and defined absorption–reflection (AR) factors among typical metals. (b) Trigger signal observed with a 100 nm Pt thin film at $\Delta f \sim 1.3$ kHz. The inset shows the rising of trigger signals measured by the ASOPS and MDL methods, where horizontal dashed lines show 20% and 80% intensities.

power change of the lights incident to the BD. R_f is the response factor, which depends on the wavelength and is estimated to be 0.16 V/mW for 400 nm light. The reflectivity change $\Delta R_{400}/R_{400}$ can be calculated by $\Delta P/P_0$, where P_0 is the power of light incident to the BD. However, the gain G decreases with the increase in the frequency of the response (for example, −3 dB at 250 kHz). Therefore, ΔP is estimated to be of the order of 1 μW for $\Delta V_{out} = 0.12$ V of the fast trigger signal, and P_0 is about 1 mW, leading to $\Delta R_{400}/R_{400} \sim 10^{-3}$.

The response speed of the signal can also be improved by using a much wider bandwidth BD. The rising time of the Pt thin film, defined as the time taken to rise from 20% to 80% intensity of its maximum, measured by the MDL method with a single laser is ~390 fs, as shown in the inset of Fig. 2(b). However, the rising time measured by the ASOPS method is ~0.4 μs, corresponding to 7 ps, which can be improved using wide bandwidth detectors. We set the gain of the BD as 1×10^3 or 1×10^4; however, the BD has the limitation of the response time and the gain decreases with the increase

in the frequency of the signal. For example, the gains decrease by -3 dB as the frequency reaches 250 and 700 kHz at 1×10^4 and 1×10^3 gains, respectively. These frequencies are defined as the bandwidth f_{BW}. The full-width at half-maximum of a pulse in the time region is estimated by $0.4/f_{BW} \sim 0.57–1.6$ μs, which corresponds to 10–30 ps. The rising time is about a half of this value, agreeing with the rising time of the trigger signal observed by the ASOPS system. Sharper trigger signals enable a higher time-resolution ASOPS measurement, and the rising time can be improved by using faster photodetectors; nevertheless, our system is capable of detecting fast dynamics up to a 100 GHz range, as discussed below.
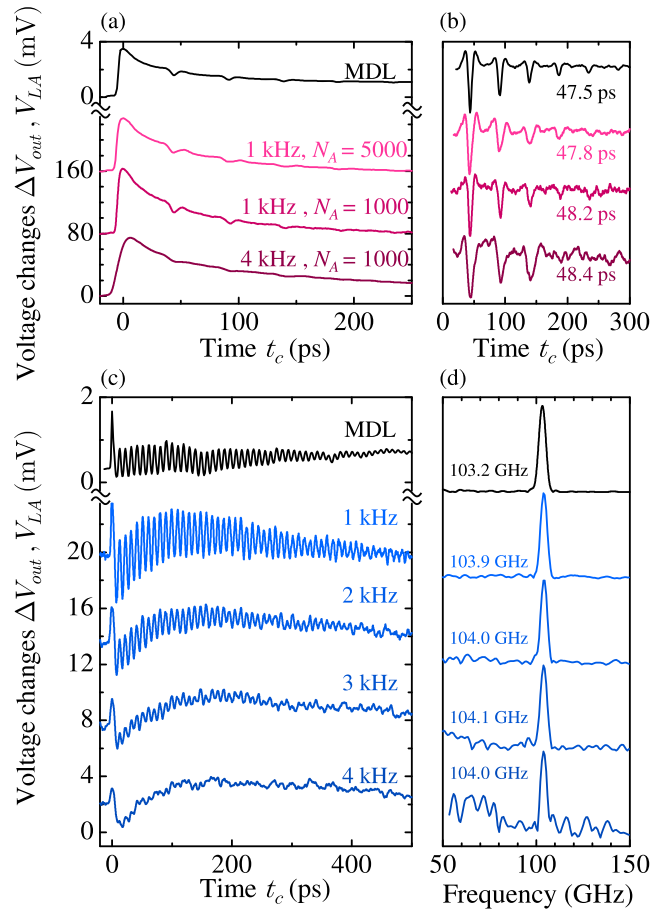
We verify the VRF-ASOPS system using two different 100 nm Pt thin films for the trigger and measurement specimens. We show raw signals in Fig. 3(a), where the color and numbers correspond to the trigger and measurement signal pairs. To obtain the signals from the measurement specimen, we use a 150-magnification apochromatic lens (Nikon, CFI TU Plan Apo EPI 150×). The powers of pump and probe lights were about 30 and 10 mW, respectively, and the gain was 10^4. The period of the trigger signal ($1/\Delta f$) fluctuates due to the drift of the cavity length caused by temperature fluctuation and mechanical vibration noise, which prevents averaging

of the measurement signals. Therefore, for each signal, we convert the observation time t_0 into actual time using each Δf^i. The converted time t_c^i is given by $t_c^i = t_o \times \Delta f^i/f_r^i$, as shown in Fig. 3(b). Here, we digitally measure the repetition frequency f_r in the PC controller. We develop a real-time-converting program that can average 1000 signals in $\sim$8 s at $\Delta f = 1$ kHz, for example.

We verify the reliability of the VRF-ASOPS method by comparing the responses obtained by the MDL and ASOPS methods. We measure acoustic echoes[49,50] in the 100 nm Pt thin film and the Brillouin oscillations[47,51] of SrTiO$_3$ as shown in Fig. 4. Δf, the average number N_A, and the powers of pump and probe lights are 1–4 kHz, 1000 or 5000 times, and 30 and 10 mW, respectively. We use the 150-magnification apochromatic lens and a 100-magnification super long working distance lens (Nikon, CFI T Plan SLWD EPI 100×) for Pt and SrTiO$_3$ measurements, respectively. In the MDL method, the maximum lock-in voltages V_{LA} are 3.7 and 1.3 mV for Pt and SrTiO$_3$ with 10^2 gain, leading to 0.5×10^{-3} and 10^{-4} reflectivity changes, respectively. On the other hand, in the ASOPS method, the maximum output voltages are 70 and 8 mV for Pt

FIG. 3. (a) Raw signals obtained from trigger and measurement specimens using 100 nm Pt thin films for both. (b) Converted and 100-times averaged signals. The color and numbers correspond to the trigger and measurement signal pairs.

FIG. 4. Comparison of MDL and VRF-ASOPS measurement with different Δf values for (a) a 100 nm Pt thin film with (b) extracted echoes and for (c) Brillouin oscillation of SrTiO$_3$ with (d) the corresponding fast Fourier transform spectra. The average number N_A for SrTiO$_3$ is 1000.

and SrTiO$_3$ with 10^3 gain, leading to about 10^{-3} and 10^{-4} reflectivity changes, respectively. In Figs. 4(b) and 4(d), the amplitudes are normalized. Measured reflectivity changes by the two methods agree with each other, insisting on the reliable measurement with high SNRs.

Importantly, our proposed system easily changes the measurement time and time resolution by changing Δf using the PZT stage in the cavity. The measurement time is inversely proportional to Δf, which falls to ~1.9 s at Δf = 4 kHz for 1000 times averaging. We detect pulse echoes every ~48 ps, as shown in Figs. 4(a) and 4(b). The measured travel times agree with each other within typical deviations of film thickness and sound velocity (a few percent). We achieve the comparable SNRs in the MDL and VRF-ASOPS measurements at Δf = 1 kHz and N_A = 5000. Small noise signals appear at Δf = 1 kHz and N_A = 1000; however, the SNR is sufficiently high to observe pulse echoes. As Δf increases, the SNR and the number of observed echoes decrease, and the acoustic pulses become broader because the increase in Δf makes the trigger signal broader, leading to the deterioration of the trigger timing. The frequency of the observed raw signals also becomes higher, and their intensities decrease because they cannot be amplified to the same gain as lower-frequency components due to the bandwidth of the BD. For example, at 1×10^3 gain and Δf = 1 kHz, a 20 GHz component corresponds to the 0.25 MHz component in the raw signal, whose normalized gain is approximately −0.30 dB. However, this corresponds to the 1 MHz component at Δf = 4 kHz, whose normalized gain becomes −4.6 dB. This bandwidth effect is significant in the Brillouin oscillation of SrTiO$_3$, as shown in Fig. 4(c). We obtain equivalent signals in the MDL and VRF-ASOPS methods at Δf = 1 kHz. However, its amplitude becomes smaller as Δf increases. Notably, SNR can be improved by using wider bandwidth detectors and increasing averaging number, and we can determine ~104 GHz frequency even at Δf = 4 kHz, as shown in Fig. 4(d). Our developed VRF-ASOPS system can be applied to imaging physical properties and making sensors using GHz ultrasound, where we can change the measurement time and time resolution depending on the objectives and purposes with appropriate bandwidth detectors.

In summary, we developed the VRF-ASOPS method without a feedback loop that can easily change the repetition frequency difference Δf, which dictates the measurement time and time resolution. Our system uses the same optics to obtain the trigger signal as the measurement specimen, realizing an easier and cheaper ASOPS system without a rigorous stabilizer, tightly tuned lasers, and specially designed programs. We show that the 100 nm Pt thin film is an excellent trigger specimen for 800 nm pump and 400 nm probe lights owing to its reflectivity, high melting point, and chemical stability. The ideal rising time of the Pt thin film is ~390 fs, which can be detected by a wider bandwidth detector. We use 250–700 kHz bandwidth balanced detectors and obtain pulse echo signals in a Pt thin film and 100 GHz Brillouin oscillations of SrTiO$_3$ by the developed VRF-ASOPS method between Δf = 1–4 kHz. Measured signals at Δf = 1 kHz are equivalent to those measured by the MDL method, and a wider bandwidth detector improves the signal quality at higher Δf. The measurement time for a 1000-time average is ~8 s, which is decreased by increasing Δf, allowing us to change the time resolution and measurement time depending on the objectives and purposes.

AUTHOR DECLARATIONS

Conflict of Interest

The authors have no conflicts to disclose.

DATA AVAILABILITY

The data that support the findings of this study are available from the corresponding author upon reasonable request.

REFERENCES

[1]C. Rønne, L. Thranea, P. O. Åstrand, A. Wallqvist, K. V. Mikkelsen, and S. R. Keiding, J. Chem. Phys. **107**, 5319 (1997).

[2]R. Ulbricht, E. Hendry, J. Shan, T. F. Heinz, and M. Bonn, Rev. Mod. Phys. **83**, 543 (2011).

[3]E. Beaurepaire, J.-C. Merle, A. Daunois, and J.-Y. Bigot, Phys. Rev. Lett. **76**, 4250 (1996).

[4]B. Koopmans, M. van Kampen, J. T. Kohlhepp, and W. J. M. de Jonge, Phys. Rev. Lett. **85**, 844 (2000).

[5]M. van Kampen, C. Jozsa, J. T. Kohlhepp, P. LeClair, L. Lagae, W. J. M. de Jonge, and B. Koopmans, Phys. Rev. Lett. **88**, 227201 (2002).

[6]C. Thomsen, J. Strait, Z. Vardeny, H. J. Maris, J. Tauc, and J. J. Hauser, Phys. Rev. Lett. **53**, 989 (1984).

[7]C. Thomsen, H. T. Grahn, H. J. Maris, and J. Tauc, Phys. Rev. B **34**, 4129 (1986).

[8]T. Tachizaki, T. Muroya, O. Matsuda, Y. Sugawara, D. H. Hurley, and O. B. Wright, Rev. Sci. Instrum. **77**, 043713 (2006).

[9]S. Kray, F. Spöler, T. Hellerer, and H. Kurz, Opt. Express **18**, 9976 (2010).

[10]Y. Kim and D.-S. Yee, Opt. Lett. **35**, 3715 (2010).

[11]P. A. Elzinga, R. J. Kneisler, F. E. Lytle, Y. Jiang, G. B. King, and N. M. Laurendeau, Appl. Opt. **26**, 4303 (1987).

[12]M. Beck, T. Plötzing, K. Maussang, J. Palomo, R. Colombelli, I. Sagnes, J. Mangeney, J. Tignon, S. S. Dhillon, G. Klatt, and A. Bartels, Opt. Express **27**, 10866 (2019).

[13]J. Cuffe, O. Ristow, E. Chávez, A. Shchepetov, P.-O. Chapuis, F. Alzina, M. Hettich, M. Prunnila, J. Ahopelto, T. Dekorsy, and C. M. S. Torres, Phys. Rev. Lett. **110**, 095503 (2013).

[14]A. Abbas, Y. Guillet, J.-M. Rampnoux, P. Rigail, E. Mottay, B. Audoin, and S. Dilhaire, Opt. Express **22**, 7831 (2014).

[15]R. Legrand, A. Huynh, S. Vincent, B. Perrin, and A. Lemaître, Phys. Rev. B **95**, 014304 (2017).

[16]G. Arregui, O. Ortíz, M. Esmann, C. M. Sotomayor-Torres, C. Gomez-Carbonell, O. Mauguin, B. Perrin, A. Lemaître, P. D. García, and N. D. Lanzillotti-Kimura, APL Photonics **4**, 030805 (2019).

[17]H. Füser, M. Bieler, S. Ahmed, and F. Verbeyst, Meas. Sci. Technol. **26**, 025203 (2015).

[18]P. Struszewski and M. Bieler, IEEE Trans. Instrum. Meas. **68**, 2295 (2019).

[19]F. Pérez-Cota, R. J. Smith, E. Moradi, L. Marques, K. F. Webb, and M. Clark, Appl. Opt. **54**, 8388 (2015).

[20]T. Dehoux, M. A. Ghanem, O. F. Zouani, J.-M. Rampnoux, Y. Guillet, S. Dilhaire, M.-C. Durrieu, and B. Audoin, Sci. Rep. **5**, 8650 (2015).

[21]F. Pérez-Cota, R. J. Smith, E. Moradi, L. Marques, K. F. Webb, and M. Clark, Sci. Rep. **6**, 39326 (2016).

[22] R. J. Kneisler, F. E. Lytle, G. J. Fiechtner, Y. Jiang, G. B. King, and N. M. Laurendeau, Opt. Lett. **14**, 260 (1989).

[23] G. J. Fiechtner, G. B. King, N. M. Laurendeau, and F. E. Lytle, Appl. Opt. **31**, 2849 (1992).

[24] G. J. Fiechtner, G. B. King, and N. M. Laurendeau, Appl. Opt. **34**, 1117 (1995).

[25] T. Yasui, E. Saneyoshi, and T. Araki, Appl. Phys. Lett. **87**, 061101 (2005).

[26] M. S. Brown, G. J. Fiechtner, J. V. Rudd, D. A. Zimdars, M. Warmuth, and J. R. Gord, Appl. Spectrosc. **60**, 261 (2006).

[27] C. Janke, M. Först, M. Nagel, H. Kurz, and A. Bartels, Opt. Lett. **30**, 1405 (2005).

[28] A. Bartels, A. Thoma, C. Janke, T. Dekorsy, A. Dreyhaupt, S. Winnerl, and M. Helm, Opt. Express **14**, 430 (2006).

[29] G. Klatt, R. Gebs, C. Janke, T. Dekorsy, and A. Bartels, Opt. Express **17**(25), 22847 (2009).

[30] A. Bartels, F. Hudert, C. Janke, T. Dekorsy, and K. Köhler, Appl. Phys. Lett. **88**, 041117 (2006).

[31] A. Bartels, R. Cerna, C. Kistner, A. Thoma, F. Hudert, C. Janke, and T. Dekorsy, Rev. Sci. Instrum. **78**, 035107 (2007).

[32] R. Gebs, G. Klatt, C. Janke, T. Dekorsy, and A. Bartels, Opt. Express **18**, 5974 (2010).

[33] G. Klatt, R. Gebs, H. Schäfer, M. Nagel, C. Janke, A. Bartels, and T. Dekorsy, IEEE J. Sel. Top. Quantum Electron. **17**, 159 (2011).

[34] T. Yasui, K. Kawamoto, Y.-D. Hsieh, Y. Sakaguchi, M. Jewariya, H. Inaba, K. Minoshima, F. Hindle, and T. Araki, Opt. Express **20**, 15071 (2012).

[35] L. Antonucci, X. Solinas, A. Bonvalet, and M. Joffre, Opt. Express **20**, 17928 (2012).

[36] L. Antonucci, A. Bonvalet, X. Solinas, M. R. Jones, M. H. Vos, and M. Joffre, Opt. Lett. **38**, 3322 (2013).

[37] L. Antonucci, A. Bonvalet, X. Solinas, L. Daniault, and M. Joffre, Opt. Express **23**, 27931 (2015).

[38] T. Hochrein, R. Wilk, M. Mei, R. Holzwarth, N. Krumbholz, and M. Koch, Opt. Express **18**, 1613 (2010).

[39] T. Hochrein, R. Wilk, M. Mei, R. Holzwarth, N. Krumbholz, and M. Koch, J. Opt. Soc. Am. B **28**, 592 (2011).

[40] R. D. Baker, N. T. Yardimci, Y.-H. Ou, K. Kieu, and M. Jarrahi, Sci. Rep. **8**, 14802 (2018).

[41] K. Tanigaki, H. Ogi, H. Sumiya, K. Kusakabe, N. Nakamura, M. Hirao, and H. Ledbetter, Nat. Commun. **4**, 2343 (2013).

[42] H. Zhang, B. Su, X. Yang, Y. Wu, J. He, C. Zhang, and D. R. Jones, Rev. Sci. Instrum. **89**, 113108 (2018).

[43] X. Yang, B. Su, Y. Wu, H. Zhang, J. He, and D. R. Jones, Meas. Sci. Technol. **30**, 045204 (2019).

[44] L. Antonucci, X. Solinas, A. Bonvalet, and M. Joffre, Opt. Express **28**, 18251 (2020).

[45] K. Uehara, H. Ogi, and M. Hirao, Appl. Phys. Express **7**, 025201 (2014).

[46] S. Iihama, Y. Sasaki, A. Sugihara, A. Kamimaki, Y. Ando, and S. Mizukami, Phys. Rev. B **94**, 020401 (2016).

[47] A. Nagakubo, A. Yamamoto, K. Tanigaki, H. Ogi, N. Nakamura, and M. Hirao, Jpn. J. Appl. Phys. **51**, 07GA09 (2012).

[48] A. Nagakubo, K. Adachi, T. Nishihara, and H. Ogi, Appl. Phys. Express **13**, 016504 (2020).

[49] H. Ogi, M. Fujii, N. Nakamura, T. Yasui, and M. Hirao, Phys. Rev. Lett. **98**, 195503 (2007).

[50] A. Nagakubo, H. T. Lee, H. Ogi, T. Moriyama, and T. Ono, Appl. Phys. Lett. **116**, 021901 (2020).

[51] H. Ogi, T. Shagawa, N. Nakamura, M. Hirao, H. Odaka, and N. Kihara, Phys. Rev. B **78**, 134204 (2008).